PROGRESS IN PHOTOVOLTAICS: RESEARCH AND APPLICATIONS
Prog. Photovolt: Res. Appl. 2009; **17**:502–512
Published online 15 May 2009 in Wiley InterScience (www.interscience.wiley.com) DOI: 10.1002/pip.905

Applications

Enhancing Thermal, Electrical Efficiencies of a Miniature Combustion-Driven Thermophotovoltaic System

Yueh-Heng Li[1], Hong-Yuan Li[1], Derek Dunn-Rankin[2*,†] and Yei-Chin Chao[1**,‡]
[1]*Department of Aeronautics and Astronautics, National Cheng Kung University, Tainan, 701, Taiwan, ROC*
[2]*Department of Mechanical and Aerospace Engineering, University of California, Irvine, CA, USA*

Methods to enhance the thermal and electrical efficiencies through novel design of combustion and thermal management of the combustor in a miniature thermophotovoltaic (TPV) system are proposed, discussed, and demonstrated in this paper. The miniature TPV system consists of a swirling combustor surrounded by GaSb PV cell arrays. The swirl combustor design, along with a heat-regeneration reverse tube and mixing-enhancing porous-medium fuel injection, improves the low illumination and incomplete combustion problems associated with typical miniature TPV systems. A reverse tube is used to enforce swirling flame attachment to the inner wall of the emitter by pushing the swirl recirculation zone back into the chamber and simultaneously redirecting the hot product gas for reheating the outer surface of the emitter. The porous medium fuel injector is used as a fuel/air mixing enhancer and as a flame stabilizer to anchor the flame. The miniature TPV system, using different combustor configurations, is tested and discussed. Results indicate that the proposed swirling combustor with a reverse tube and porous medium can improve the intensity and uniformity of the emitter illumination, and can increase the thermal radiant efficiency. Consequently, the overall thermal efficiency and electrical output of the miniature TPV system are greatly enhanced. Copyright © 2009 John Wiley & Sons, Ltd.

KEY WORDS: thermophotovoltaic power generator; radiant efficiency; thermal efficiency; porous medium

Received 27 November 2008; Revised 24 March 2009

INTRODUCTION

The fact that traditional batteries fail to satisfy the rapidly growing needs for higher energy/power density devices for mesoscale and microscale electromechanical systems has encouraged the search for advanced and reliable portable and miniaturized high-density power sources. It has been shown[1] that hydrocarbon fuels, with their high energy/power density, have favorable properties for powering miniature and micro systems. In the process of miniaturizing hydrocarbon-fueled power systems, however, increasing surface-to-volume (S/V) ratio can lead to incomplete combustion and flame instability.[2–3] Some logical strategies have been developed to overcome these challenges, such as

* Correspondence to: Derek Dunn-Rankin, Department of Mechanical and Aerospace Engineering, University of California at Irvine, Irvine, California 92697, USA.
† E-mail: ddunnran@uci.edu
** Correspondence to: Y. Chao, Institute of Aeronautics and Astronautics, National Cheng Kung University, No.1, Ta-Hsueh Rd., Tainan, 701, Taiwan, ROC.
‡ E-mail: ycchao@mail.ncku.edu.tw

using quench-resistant fuels, liquid-fuel-film combustors,[4–6] high-preheat concepts (as with the Swiss-roll burner[7]), and catalytic surfaces.[8] Among these novel and viable small-scale power source designs, the thermophotovoltaic (TPV) power system promises to be a very clean and quiet source of electrical power with no moving parts and high power density, using a wide variety of fuels.[9–12] In general, small-TPV power systems consist of a combustor, with its wall serving as an emitter, and a PV array. The system is simple yet effective.

On the other hand, the most obvious drawbacks of TPV power devices are their low conversion efficiency and low throughput. The overall efficiency of a conventional TPV power system is the product of the efficiencies of the PV cells and the radiation source, with the latter consisting of the combustor and the emitter. For improving the overall efficiency of TPV power systems, most researchers emphasize the improvement and development of novel and viable materials for PV cells and radiant emitters. In particular, technological improvements in the fields of selective emitter and low band gap PV cells have opened a new page for TPV generation of electricity.[13–16] Despite material limitations, both combustor and emitter are key components in the design of any small-scale TPV power device. Usually, the emitter serves both to confine the combustion and to convert heat transferred from the flame into emitted radiation. As regards small-scale combustors, their design is highly constrained by short residence time for complete combustion and high rates of heat dissipation through the combustor wall. Therefore, the major challenge in small-scale combustor design is to maintain an optimal balance between sustaining combustion and maximizing the heat output. A high surface-to-volume ratio (S/V) is very favorable for output power density per unit volume but a high heat output may compromise stable combustion. This is because heat loss through the combustor wall increases rapidly with S/V ratio, which tends to suppress flame ignition and to quench the reaction. Not only does the high heat loss decrease the chemical efficiency of the combustion, but it also deactivates chemical reactions by lowering the flame temperature. The coupling between fluid dynamics, heat transfer, and chemical kinetics is therefore much more prominent as system size decreases, making this coupling a critical criterion in the design process.[17]

In view of the drawbacks and deficiencies of conventional TPV power systems discussed above, it is desirable to look further into the design of a combustor capable of rendering high and uniform temperature and high-intensity illumination along the combustor wall/emitter to enhance the radiation and thermal efficiency. This paper presents a combustor design with a transparent heat-regeneration reverse tube and a mixing-enhancing porous-medium fuel injector that improves the low illumination and incomplete combustion problems associated with miniature TPV systems. The combustor design and performance are further examined and discussed in the following sections.

EXPERIMENTS

Combustor, emitter and photovoltaic cells

A combustion-driven TPV power system usually consists of a combustor/thermal radiator coupled with PV cell arrays. In this paper, the radiant combustor is investigated in an attempt to maximize the radiation output and radiant efficiency. The radiant combustor consists of a main combustion chamber (9.5 mm inside diameter (ID) and 60 mm length) with swirling air inlet ports. The chamber is set with a fuel trough of 6 mm ID and fuel inlet ports, as shown in Figure 1(a). For experiments, two kinds of combustion chamber materials are used, an infrared thermal tube (ZrO_2) for enhanced thermal radiation conversion and a quartz tube for visualization. The infrared thermal tube (ZrO_2) is used as a broadband emitter for the TPV system and operates effectively in the temperature range 1000–1600 K. The combustor is designed as a conventional swirling combustion type where a fully aerated swirl flame is stabilized in the combustor close to the combustor surface (which is the emitter), heating the surface to incandescence.

Instrumentation

As shown schematically in Figure 1(b), methane is metered by an electronic flowmeter calibrated in the range of 0–5 slpm, and dry compressed air is provided from an air compressor and then metered by an electronic flowmeter calibrated in the range of 0–60 slpm. For temperature measurements, exit product gas temperature is measured by an R-type thermocouple with 75-μm bead diameter with an uncertainty of $\pm 20^{\circ}$C, and the surface temperature of the emitter is detected by an infrared thermometer with an uncertainty

DOI: 10.1002/pip

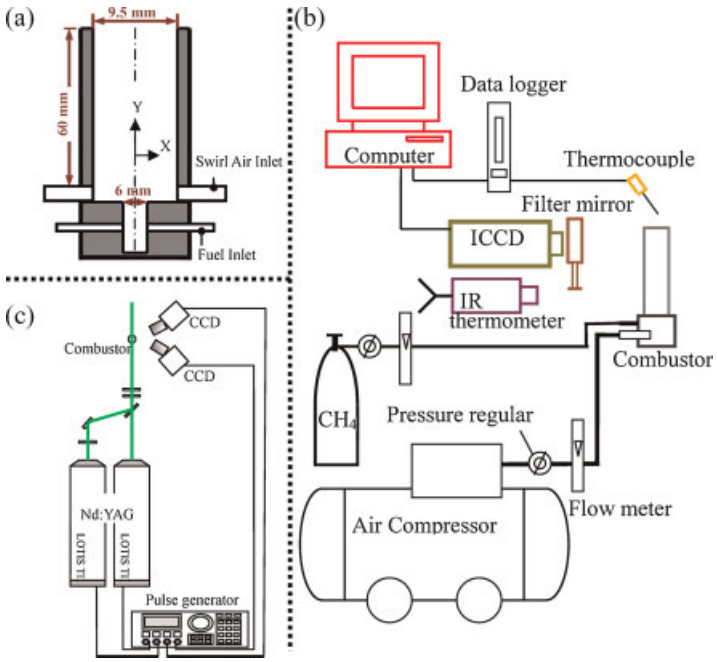

Figure 1. Schematic diagram of the experimental combustor (a), schematic diagram of the experimental setup (b), and stereo PIV measurement system (c)

of $\pm$ 10°C. The infrared thermometer used in this study is Model MA2SC with close focus optics and laser aiming produced by Raytec Non-contact Infrared Temperature Measurement. The optimized measuring temperature range is from 623 to 2273 K, optical resolution is more than 300:1 with standard focus and spectral response is 1.6 μm. Furthermore, flame chemiluminescence images are taken through a 14-bit intensified CCD camera with narrow bandpass filters (10 nm FWHM) at wavelengths of 307 nm for OH^*, 430 nm for CH^*, and 515 nm for C_2^*.

The stereo particle image velocimetry (PIV) system, consisting of two CCD cameras (1280 × 1024 pixels), two pulse Nd:YAG lasers, and a synchronizing pulse generator, is used to map the velocity profile of the swirling combustor flowfield in the current TPV system, as shown in Figure 1(c). The angular-displacement stereo PIV method is employed. The lenses of the cameras are rotated inwards such that their axes intersect at the mid-point of the recorded image to reduce geometric distortion due to misalignment of the object plane relative to the lens plane. To overcome this problem, the Scheimpflug condition that requires the object, the lens, and the image planes to intersect at a common line, is applied. This arrangement introduces a strong perspective distortion and magnification factor variation across the image plane. These issues are resolved by software image reconstruction. Gas emissions are examined by using a gas analyzer (MRU). Concentration of NO_x is calibrated in the range of 0–5000 ppm with an uncertainty of $\pm$ 2 ppm; CO concentration is calibrated in the range of 0–10 000 ppm with an uncertainty of $\pm$ 20 ppm.

ENHANCEMENT APPROACHES

Swirling air system

As described earlier, miniaturization of the combustion configuration often results in problems associated with reduced length scale, such as increased S/V, less air/fuel mixing, and reduced residence time. These effects can lead to incomplete combustion and flame instability, which further diminish the radiant efficiency of the emitter and overall thermal efficiency of the miniature combustor. Nevertheless, swirling flow systems have generally been used in small chambers to enhance fuel/air mixing, increase residence time, and induce flow recirculation for flame stabilization. In the

DOI: 10.1002/pip

present study, tangential air inlets are utilized in the chamber to generate swirl flow. In order to estimate the swirling flow structure generated by the swirl, stereo PIV is employed to measure 3D velocities in the vicinity of the chamber exit. In Figure 2(a), arrows represent the averaged u–v velocity field and the background color represents the averaged w velocity component. Results show that the tangential velocity component w is of the same order as the axial velocity component v, but is larger than the radial velocity component u by about one order of magnitude. Noticeable reversed-flow velocity vectors can be found in the centerline near the combustor exit, indicating the existence of a large recirculation zone which squeeze into the chamber. Existence of the recirculation zone provides clear evidence of enhancement of the residence time, fuel/air mixing and flame stabilization in the miniature combustor.

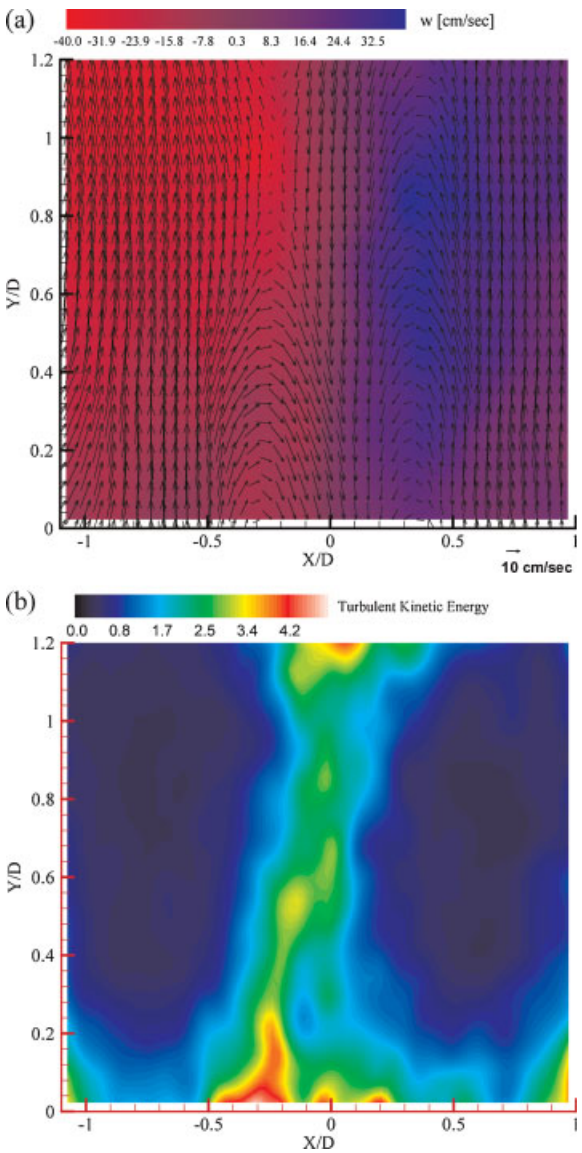

Figure 2. 3D PIV measurement results at the chamber exit without the reverse tube in the air flow condition of 8.5 slpm, (a) average velocity distribution and (b) turbulent kinetic energy distribution in the vicinity of the chamber exit

An indication of the fuel/air mixing in this flow is given by the turbulent kinetic energy, k_T, defined as: $k_T = \frac{1}{2}\sqrt{\left(\overline{u'^2} + \overline{v'^2} + \overline{w'^2}\right)}$, where $\overline{u'^2}$is the mean value of the squared fluctuation in the x-direction, $\overline{v'^2}$ in the y-direction, and $\overline{w'^2}$in the z-direction. Figure 2(b) shows the kinetic energy k averaged over 300 stereo PIV images. High turbulent kinetic energy levels, indicating high probability of good fuel/air mixing, are found to congregate in the recirculation region. The most intense turbulent mixing in this flow field occurs in the vicinity of the chamber exit, and its value reaches about 5%. Therefore, the present swirling flow can effectively generate a recirculation zone in the center extending to the exit of the chamber. To further define the degree of swirl in the flow, the swirl number S is introduced as: $S(z) = \frac{G(y)/2}{1-(G(y)/2)}$ and $G(y) = \frac{w_{\max}(y)}{v_{\max}(y)}$, where $w_{\max}(y)$ and $v_{\max}(y)$ are, respectively, the maximum w and v velocities measured at a distance y from the chamber exit. From the stereo PIV results, the v and w velocity profiles can be extracted at different heights (see Figures. 3(a–b)). The axial and tangential velocity profiles at the chamber exit in Figure 3 depict a typical swirling recirculation flowfield with high axial and tangential velocities near the wall (X/D $= \pm 0.5$), and high reverse axial and almost zero tangential velocities on the centerline. The swirl numbers at the exit along the axial direction shown in Figure 3(c) are above 0.6 and represent strong swirling flow capable of generating a central recirculation, according to Gupta *et al.* [18]

Uniform and high intensity illumination is essential for an emitter to have a high radiant efficiency. Emitter radiant efficiency is strongly related to surface temperature of the emitter. Figure 4 exhibits the illumination feature of the conventional swirling combustor in operation. It appears that the emitter illumination is not uniform but is congregated in the lower section of the emitter. Hence, although flames can be stabilized inside the combustion chamber by a swirling system, the non-uniform illumination of the

DOI: 10.1002/pip

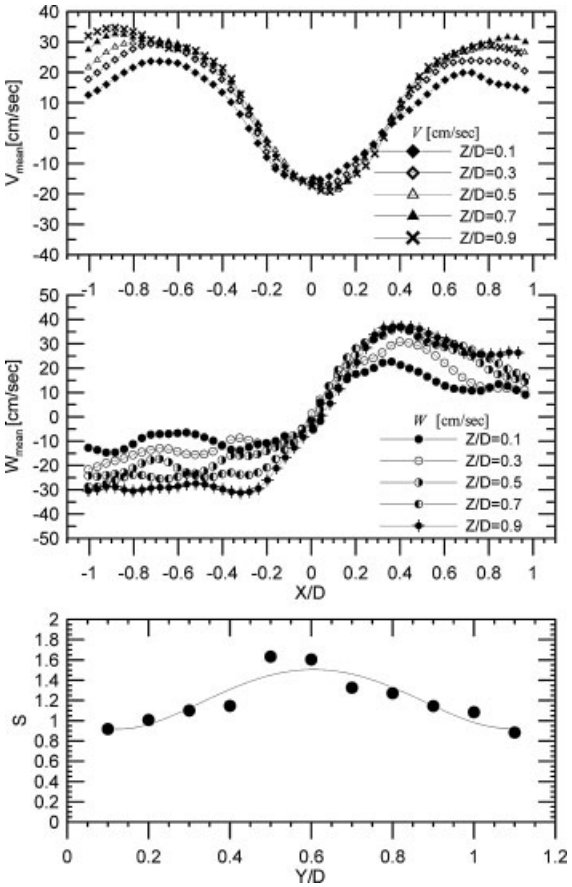

Figure 3. Profiles for (a) *v* and (b) *w* velocity distribution at varied positions as well as (c) the swirl number along axis direction

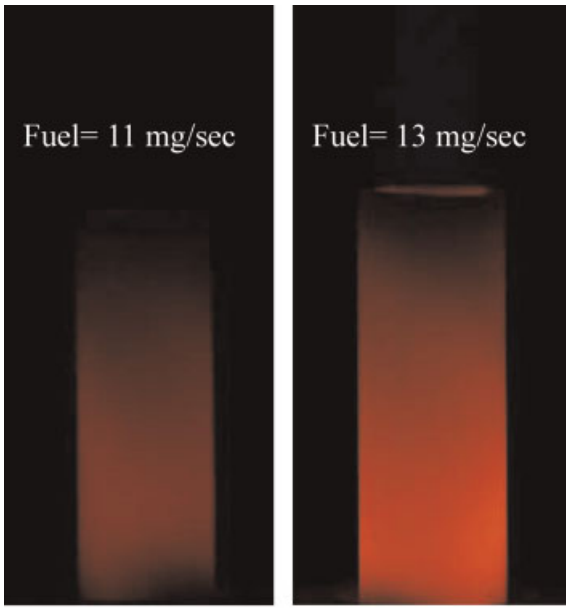

Figure 4. Photographs of combustion chamber operation in different fuel input conditions

emitter may diminish the radiant efficiency and the overall efficiency of the small PTV power system.

The reverse tube

To remedy this non-uniform emitter illumination problem, a heat-regenerating reverse tube is implemented for redirecting the hot product gas to reheat the emitter. Figure 5(a) displays a schematic diagram of the combustor with a reverse tube (without a porous cap), and Figure 5(b)–(c) show photographs of the experimental combustor assembly and set-up. The parameter *D* labeled in Figure 5(a) defines the distance between the top of the reverse tube and the combustor exit. The reverse tube is made of quartz and its inner diameter is 22 mm. There are four exit tubes at the bottom of the reverse tube for exhausting product gas. The main function of the reverse tube is to redirect hot product gas to pass through the chamber and reheat the emitter. However, the existence of the reverse tube may also push the recirculation zone further into the chamber, which forces the swirl flame to further cling to the wall. In this case, the emitter can attain thermal energy more efficiently by means of heat transfer from the flame as well as the redirected hot product gas.

Images in Figure 6 exhibit the intensity and uniformity of illumination from the emitter for different thermal inputs and distance *D* conditions with an exposure time of 1/20 s. Comparison between Figure 6(a–b), for two *D* values and constant fuel mass flow rate ($11\,\mathrm{mg\,s^{-1}}$) and equivalence ratio (ER = 0.85), shows that the illumination of the emitter is similar and the uniformity of both emitters is equal. If the fuel mass flow rate is increased to $13\,\mathrm{mg\,s^{-1}}$ (with constant equivalence ratio), strong swirling flow upstream forces the flame to recede downstream. Consequently, the lack of flame stabilization and inadequate fuel/air mixing produces a dark area in the lower section of the emitter, as shown in Figure 6(c–d). In order to quantify the uniformity of illumination, surface temperature along the emitter is measured by IR thermometry. Figure 7 exhibits the temperature distribution along the emitter for cases of fixed ER and varied fuel inputs. Apparently, an emitter with a

DOI: 10.1002/pip

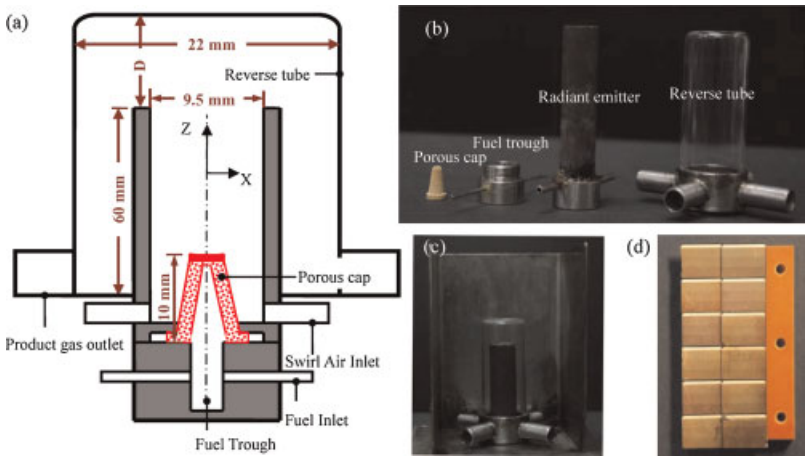

Figure 5. Schematic diagram of the experimental combustor with a reverse tube/porous medium (a), photographs of each part of the experimental combustor (b), prototype TPV power system setup (c), and a PV cells array (d)

reverse tube has higher surface temperature than it has without a reverse tube. Furthermore, when the fuel mass flow rate reaches $11\,mg\,s^{-1}$, the surface temperature distribution becomes uniform and its value reaches around 880°C. A change in distance D does not significantly affect the illumination intensity in the relatively low swirling air condition. When the fuel mass flow rate rises to $13\,mg\,s^{-1}$, surface temperature near the chamber exit increases to 1000°C. The surface temperature difference along the emitter also becomes prominent, varying from 880°C in the upstream to near 1000°C near the exit, in the relatively high swirling air condition. Decreasing the distance D contributes slightly to changes in surface temperature.

The overall efficiency of the TPV power system is related to combustion and heat transfer efficiencies of the combustion chamber and radiant efficiency of the emitter. In order to monitor the combustion efficiency of the present combustion system, measurements are conducted using a gas analyzer to obtain CO_2, CO, O_2, and unburned hydrocarbons (UHC) concentrations in the product gas. The combustion efficiency for methane fuel can be defined as the ratio of the measured volume percentage between carbon dioxide and all carbon-containing species, including CO_2, CO, and UHC. Figure 8 displays the CO and NO_x emissions referred to 15% O_2 for varied equivalence ratios and fixed fuel mass flow rate ($11\,mg\,s^{-1}$). In the case without a reverse tube, CO emission rises when the fuel flow rate is increased, and its value ranges between 450 and 750 ppm. However, the corresponding NO_x does not change significantly. Combustion efficiency can reach 98% for all the cases tested. Nevertheless, the case with a reverse tube has an obvious change of CO emission. In the fuel-lean condition, CO emission is low with a value below 100 ppm. As the equivalence ratio increases, CO emission jumps sharply and even exceeds the case without a reverse tube. An increase in the equivalence ratio with fixed fuel flow rate requires a decrease in the air flow rate, which consequently reduces the swirling intensity. Low swirling flow reduces the fuel/air mixing and brings about incomplete combustion. Therefore, the combustion efficiency reduces to 91.5% when the equivalence ratio approaches fuel-rich conditions.

Conventionally, the radiant efficiency of the emitter is estimated by the ratio of net radiation power from the emitter to the heating value of the fuel. However, not all the heating value of fuel transfers to the emitter as some energy is carried away by the exhaust gas. The net amount of energy absorbed by the emitter can be defined as the difference between the heating value of the fuel input and the remnant thermal content of the exhaust gas. The remnant thermal content of the exhaust gas can be evaluated by measuring the exhaust gas temperature and its composition. Table I shows the radiant efficiency for the conditions of equivalence ratio 0.85 and 1.0, under different combustion configurations. In the case of the emitter without a reverse tube, the radiant efficiency is 5.82% for an equivalence ratio of 1.0 and 6.22% for an equivalence ratio of 0.85. It appears that the radiant efficiency of the conventional combustor is dominated by the intensity

DOI: 10.1002/pip

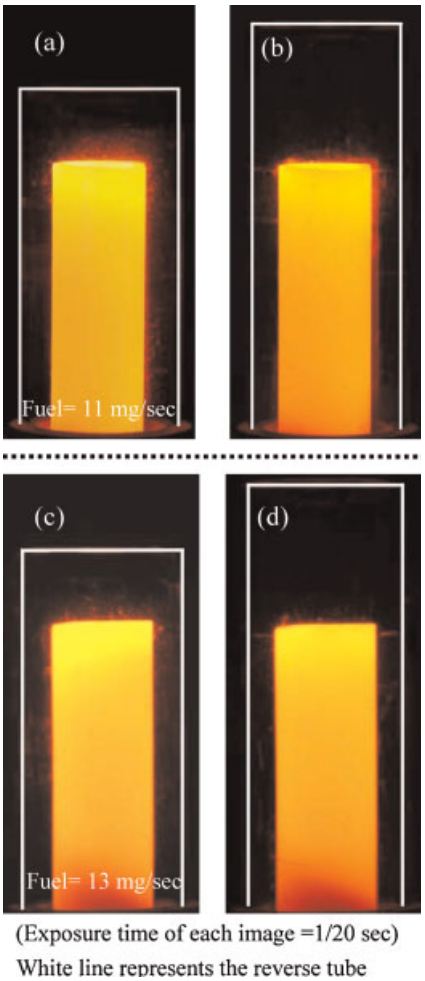

Figure 6. Photographs of combustion chamber operation with a reverse tube using 11 mg s^{-1} fuel flow input and distance $D = 1$ cm(a) and 2 cm(b), and 13 mg s^{-1} fuel flow input and distance $D = 1$ cm(c) and 2 cm(d)

of the swirling flow. Stronger swirling air (which for the present case means lower equivalence ratio, as the fuel flow rate is fixed) produces good fuel/air mixing which confines the flame inside the chamber and thereby enhances the heat transfer to the emitter. Adding a reverse tube further increases the radiant efficiency, which reaches 6.42% for an equivalence ratio of 1.0 and 7.60% for an equivalence ratio of 0.85. Hence, the novel design of the reverse tube improves both the combustion and radiant efficiencies.

Porous medium

As shown above, low swirling air diminishes fuel/air mixing and reduces combustion efficiency, and strong

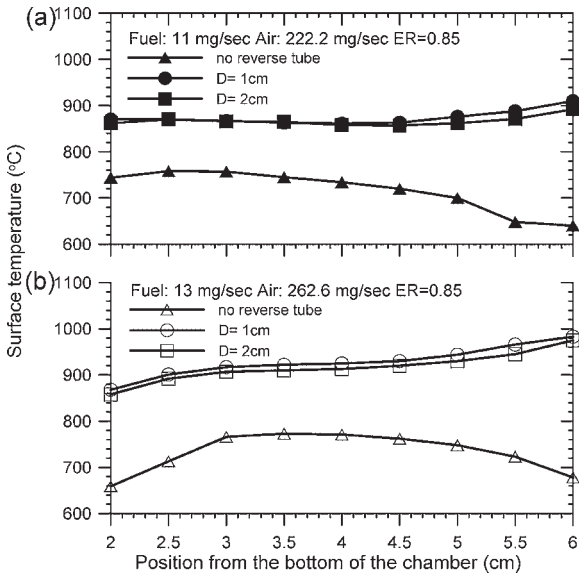

Figure 7. Measured wall temperature distribution in the axial direction for fuel flow of (a) 11 mg s^{-1} and (b) 13 mg s^{-1} with/without a reverse tube

swirling air shifts the flame anchoring position downstream, resulting in dark areas on the emitter. Therefore, a porous medium in the combustor is proposed to promote fuel/air mixing and stabilize the flame. Figure 5(a) displays a schematic diagram of the combustor with a reverse tube and a porous medium. The porous medium is made of bronze material. It has a truncated conical shape of 4 mm diameter on top, 6.5 mm diameter on the bottom, and 10 mm long. The pore size is approximately 20 μm. Fuels are allowed to flow into the chamber only through the peripheral surface, but not through the top flat. This type of fuel injection can be categorized with the asymmetric whirl concept.[19] In an asymmetric whirl, the fuel is injected off-axis of a swirling air flow in order to enhance fuel/air mixing.

Figure 9 shows the CO and NO_x emissions for various equivalence ratios at a fixed fuel flow rate (11 mg s^{-1}). There is no apparent difference in CO emission in the fuel-lean condition for the combustors with and without a porous medium. When the equivalence ratio approaches stoichiometric and fuel-rich conditions, also a relatively low swirling air condition, CO emission of the combustor with the porous medium significantly decreases by 500 and 1500 ppm for stoichiometric and fuel-rich conditions respectively, as compared to the combustor without a porous medium. Correspondingly, the combustion

DOI: 10.1002/pip

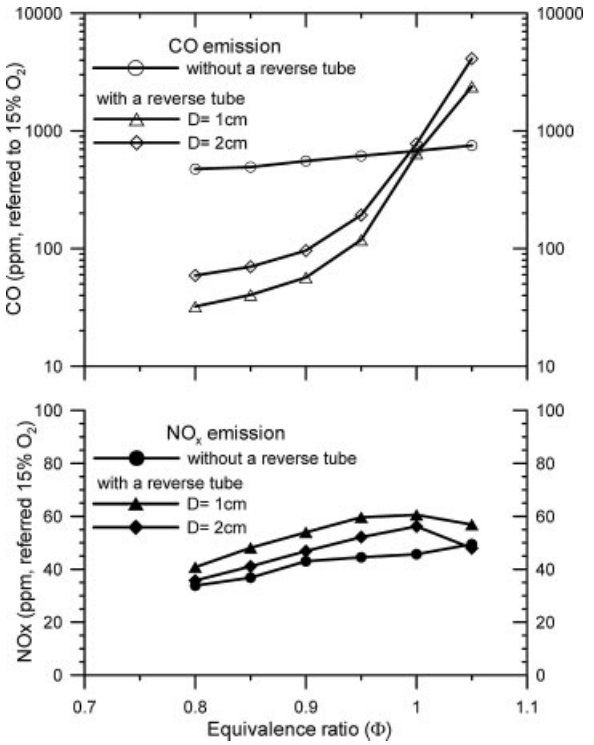

Figure 8. Effect of equivalence ratio and distance D on (a) CO and (b) NO_x emissions

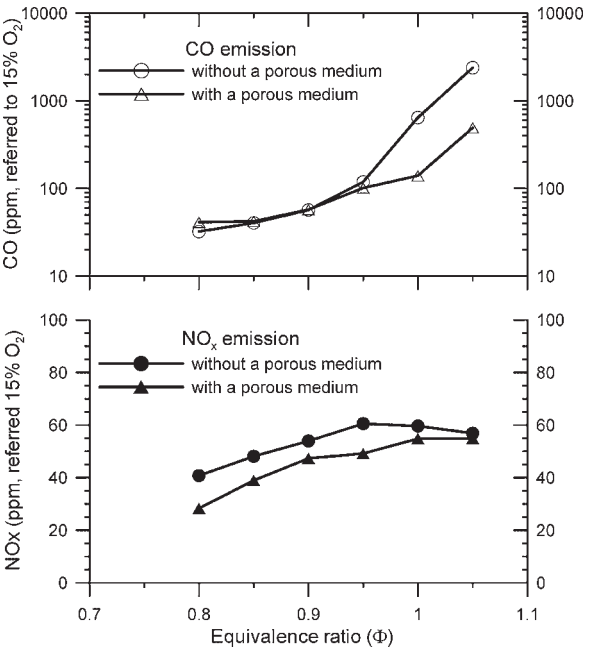

Figure 9. Effect of equivalence ratio and porous medium on (a) CO and (b) NO_x emissions

efficiency of the combustor with the porous medium can reach 98% even when operated with an equivalence ratio of 1.05. This is because the porous medium enhances fuel/air mixing, which further increases the combustion efficiency, especially for low swirling air conditions.

As regards the emitter illumination, one can find for low swirling air conditions (11 mg s^{-1} fuel mass flow rate and 1.0 equivalence ratio) that the illumination of the emitter is similar with or without the porous medium, as shown in Figure 10(a–b), respectively. However, for high swirling air conditions (13 mg s^{-1} fuel mass flow rate and 0.85 equivalence ratio), there is a dark area in the lower section of the emitter for the combustor without a porous medium (see in Figure 10(d)). In the case with a porous medium, the uniformity and intensity of the illumination of the emitter are significantly improved (seen in Figure 10(c)). Hence, it appears that adding a porous medium not only improves the fuel/air mixing but also acts as a flame stabilizer. Figure 11 indicates the surface temperature along the emitter under different fuel input conditions. For the conditions of 11 mg s^{-1} fuel flow rate and 1.0 equivalence ratio, the emitter illumination of the combustor with a porous medium

Table I. Radiant efficiencies in different conditions

Equivalence ratio	Distance D (cm)	Thermal input (W)	Remnant gas energy (W)	Radiant energy (W)	Radiant efficiency (%)
1.0[a]	NO	611.6	252.45	20.92	5.82
1.0[a]	1	611.6	106.81	32.40	6.42
1.0[b]	1	611.6	109.15	32.97	6.56
0.85[a]	NO	611.6	248.5	22.58	6.22
0.85[a]	1	611.6	103.59	38.62	7.60
0.85[b]	1	611.6	118.33	39.56	8.02

[a]the combustor without a porous cap.
[b]the combustor with a porous cap.

DOI: 10.1002/pip

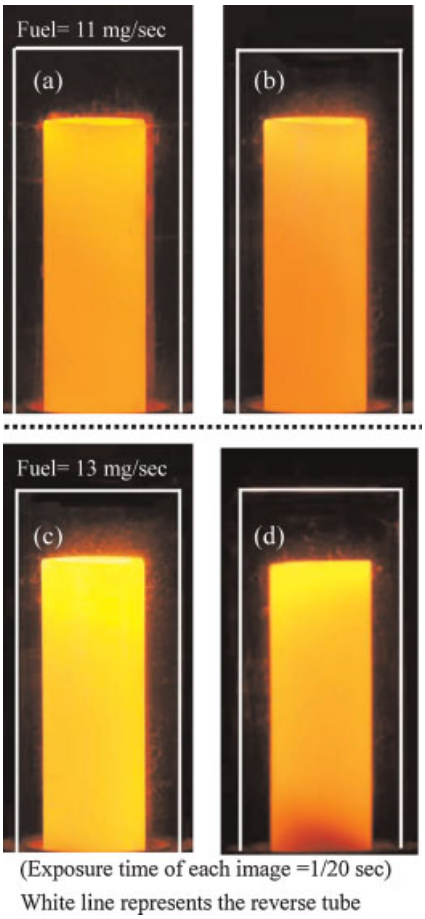

Figure 10. Photographs of combustion chamber operation with a reverse tube using fuel flow of 11 mg s^{-1} with a porous medium (a) and without a porous medium (b), and with fuel flow of 13 mg s^{-1} with a porous medium (c) and without a porous medium (d)

has slightly higher temperature in its lower section than that of the combustor without a porous medium, as shown in Figure 11(a). It is evident that a porous medium can ameliorate the lack of fuel/air mixing in fuel-rich and low swirling air conditions. Moreover, in the conditions of 13 mg s^{-1} fuel flow rate and 0.85 equivalence ratio, the surface temperature of the combustor with a porous medium ranges between 970 and 1000°C, which is higher than that of the combustor without a porous medium, as shown in Figure 11(b). The pronounced difference indicates that the porous medium effectively stabilizes the flame in the bottom of the chamber under relatively strong swirling air conditions, which ensures stable flame heating of the emitter in the upstream region. In terms of radiant efficiency, the combustor with the porous medium can

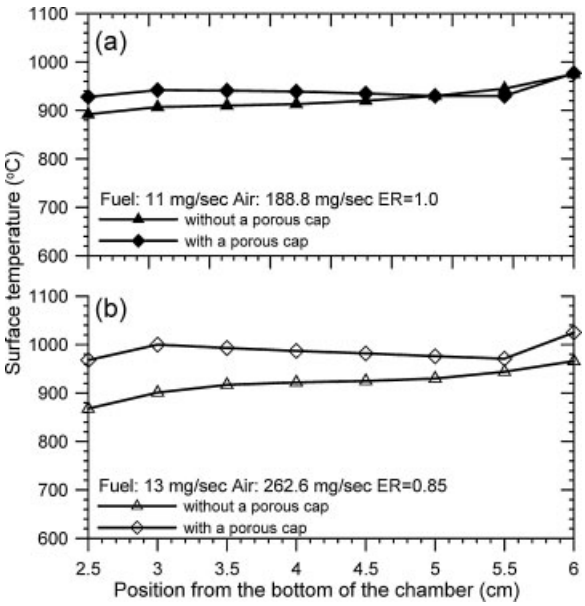

Figure 11. Measured wall temperature distribution in the axial direction for equivalence ratio of (a) 1.0 and (b) 0.85 with/without a porous medium

reach 6.55% for an equivalence ratio of 1.0 and 8.02% for an equivalence ratio of 0.85. These results show that a porous medium further enhances the radiant efficiency by improving the fuel/air mixing and flame stabilization in the present TPV power system.

In order to visualize and verify the flame structure inside the chamber, the infrared thermal tube is replaced by a quartz tube. The flame structure can be monitored through the transparent reverse tube and quartz tube. Figures 12(a–c) show flame photographs inside the chamber for the conditions with a porous medium and without a porous medium, respectively. For the case without a porous medium, the flame inclines to the central line of the combustion chamber. In contrast, the flame with a porous medium leans toward the combustor wall. OH^* chemiluminescence images for both cases are taken and transformed by Abel deconvolution,[20] as shown in Figure 12(b–d). These chemiluminescence images represent the flame structure and its corresponding flame position. Figure 12(c) indicates that the high OH^* radical intensity is confined in a thin layer inclined to the central line and it congregates in the base of the chamber. Thus it means that the flame layer (reaction zone) converges to the central line of the chamber in the case without a porous medium, as for a typical jet flame. However, OH^* distributes along the combustor wall for the case with a porous medium. Methane is

DOI: 10.1002/pip

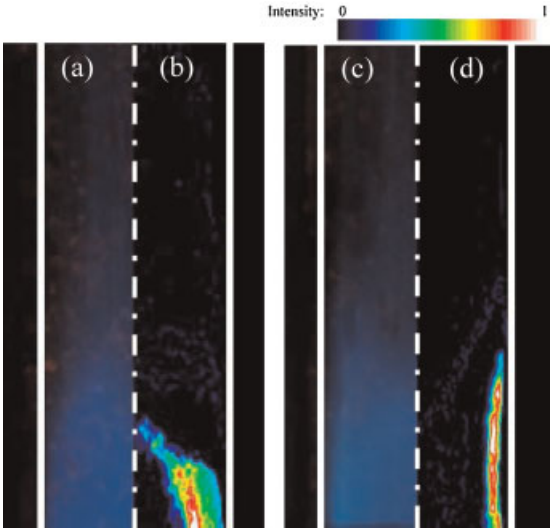

Figure 12. Images of the flame structure and corresponding OH radial distribution inside the chamber in the cases without (a), (b), and with (c), (d) a porous medium

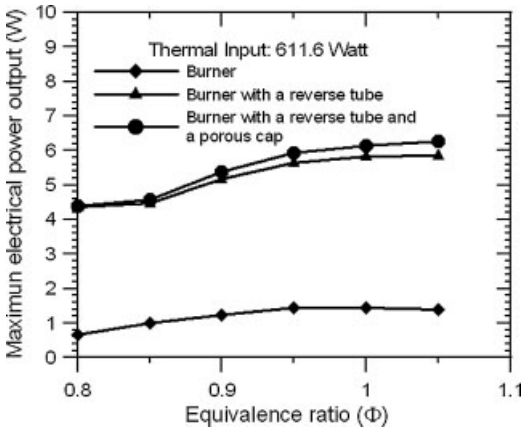

Figure 13. The maximum electrical power output under different equivalence ratios of methane for three kinds of combustors

injected peripherally through the porous medium so that it can be quickly mixed with the swirling air. Consequently, the flame burns along the combustor wall, providing optimal transfer of thermal energy to the emitter. This flame/wall interaction means that the emitter with a porous medium produces high and uniform illumination.

Systematic efficiency demonstration

In order to evaluate the benefit of improving the miniature combustion-driven TPV system, GaSb PV cells are employed to collect illumination emission and convert it into electricity. The prototype TPV system consists of the miniature combustor with necessary assemblies surrounded by four PV cell modules. Each cell array has an area of 18 cm^2 and contains two strings of 6 series connected cells in parallel, as shown in Figure 5(d). The electrical power output of the prototype mesoscale TPV system incorporating GaSb cell modules is then measured for various equivalence ratios and different combustor configurations as shown in Figure 13. With identical thermal input, maximum electrical power output of the conventional burner increases depending upon the equivalence ratio. As fuel/air ratio moves toward the stoichiometric condition, power output correspondingly increases due to stable and complete combustion. After annexing the reverse tube, the electric power output increases by more than a factor of 4. The maximum power output can reach 5.84 W when the ER is slightly rich at 1.05, and its overall efficiency is approximately 0.95%. Furthermore, when utilizing a porous medium to improve the fuel/air mixing, further enhancement of the electric output and efficiency can be achieved. For an equivalence ratio of 1.05, an electrical power output of 6.27 W is achieved for the small TPV system, corresponding to an overall efficiency of 1.02%, which is higher than that reported previously.[11] The open-circuit voltage and short-circuit current are 1.81 V and 6.6 A respectively. The fill factor reaches 0.0.525. The high efficiency region of the GaSb PV cell spans between 600 and 1700 nm in wavelength, but most of the output from the present emitter ranges between 1300 and 2100 nm. The non-matching photons are not converted into electricity by PV cells, and this loss of photons is one of the main contributions to the low efficiency of current TPV systems. In order to further improve the efficiency of the small TPV system, it is necessary to employ a lower band gap of GaInAsSb PV cells, where high quantum efficiency is achieved in the ranges between 800 and 2400 nm. Furthermore, by utilizing a selective emitter to replace the present infrared thermal broadband emitter, most of the photons emitted can be located in the short wavelength range with energies greater than the bandgap of the PV cells. With such a change, the efficiency is expected to increase significantly. In addition, the exhaust product gas possesses a large amount of thermal energy which is lost to the ambient. Effectively extracting the energy from the exhaust product gas by using thermoelectric materials may be an approach to improve the overall efficiency even further.

DOI: 10.1002/pip

CONCLUSION

Novel methods to effectively improve the electric output and thermal efficiency of a mesoscale combustion-driven TPV system are proposed and tested. A swirling air system is used to increase the residence time, enhance fuel/air mixing, and stabilize the flame in the miniature combustor. The illumination of the emitter; however, is non-uniform and has low intensity due to low heat transfer. In order to ameliorate this situation, a reverse tube is demonstrated that redirects hot products to reheat the emitter. With the reheat, the results show that the chamber wall has uniform illumination and that the flame can be confined inside the chamber. Nevertheless, under high air flow rate conditions the flame may be forced to recede downstream by strongly swirling air so that a dark area appears in the low section of the emitter. At the same time, strongly swirling air moderates the fuel/air mixture which then reduces the chemical efficiency, especially under fuel-rich conditions. Consequently, a porous medium was implemented to enhance the fuel/air mixing and to double as a flame holder. In the process of improvement, the overall efficiency was increased by more than a factor of 4, from 0.24 to 1.02%. For a practical portable TPV system, some non-power means of fuel-air feeding system are usually considered, such as a pre-pressurized bottle and a vaporization pumping system etc. In this way, reducing the operational power required is feasible and reliable.

REFERENCES

1. Dunn-Rankin D, Leal EM, Walther DC. Personal power system. *Progress in Energy and Combustion Science* 2005; **31**: 422–465.
2. Fernandez-Pello AC. Micropower generation using combustion: Issues and approaches. *Proceedings of the Combustion Institute* 2003; **29**: 883–899.
3. Ameel TA, Papautsky I, Warrington RO, Wegeng RS, Drost MK. Miniaturization technologies for advanced energy conversion and transfer systems. *Journal of Propulsion and Power* 2000; **16**: 577–582.
4. Li YH, Chao YC, Dunn-Rankin D. Combustion in a meso-scale liquid-fuel-film combustor with central-porous fuel inlet. *Combustion Science and Technology* 2008; **180**: 1900–1919.
5. Li YH, Chao YC, Sarzi Amadé N, Dunn-Rankin D. Progress in miniature liquid film combustors: Double chamber and central porous fuel inlet designs. *Experimental Thermal and Fluid Science* 2008; **32**: 1118–1131.
6. Li YH, Chao YC. Development of a meso-scale central-porous-fuel-inlet combustor, VDM Verlag Dr. Muller Aktiengesellschaft & Co. KG., 2008.
7. Ahn J, Eastwood C, Sitzki L, Ronney PD. Gas phase and catalytic combustion in heat recirculating burners. *Proceedings of the Combustion Institute* 2005; **30**: 2463–2472.
8. Chao YC, Chen GB, Leu TS, Wu CY, Cheng TS. Operational characteristics of catalytic combustion in a platinum microtube. *Combustion Science and Technology* 2004; **176**: 1755–1777.
9. Basu S, Chen YB, Zhang ZM. Microscale radiation in thermophotovoltaic devices - A review. *International Journal of Energy Research* 2007; **31**: 689–716.
10. Chia LC, Feng B. The development of a micropower (micro-thermophovoltaic) device. *Journal of Power Sources* 2007; **165**: 455–480.
11. Qiu K, Hayden ACS. Thermophotovoltaic power generation systems using natural gas-fired radiant burners. *Solar Energy Materials and Solar Cells* 2007; **91**: 588–596.
12. Yang WM, Chou SK, Shu C, Xue H, Li ZW. Development of a prototype micro-thermophotovoltaic power generator. *Journal of Physics D: Applied Physics* 2004; **37**: 1017–1020.
13. Ferguson LG, Dogan F. A highly efficient NiO-doped MgO matched emitter for thermophotovoltaic energy conversion. *Materials Science and Engineering B* 2001; **83**: 35–41.
14. Bitnar B, Durisch W, Mayor J-C, Sigg H, Tschudi HR. Characterisation of rare earth selective emitters for thermophotovoltaic applications. *Solar Energy Materials and Solar Cells* 2002; **73**: 221–234.
15. Yang WM, Chou SK, Shu C, Li ZW, Xue H. Research on micro-thermophotovoltaic power generators. *Solar Energy Materials and Solar Cells* 2003; **80**: 95–104.
16. Wang CA, Choi HK, Ransom SL, Charache GW, Danielson LR, DePoy DM. High-quantum-efficiency 0.5 eV GaInAsSb/GaSb thermophotovoltaic devices. *Applied Physics Letters* 1999; **75**: 1305–1307.
17. Mehra A, Zhang X, Ayon AA, Waitz IA, Schmidt MA, Spadaccini CM. A six-wafer combustion system for a silicon micro gas turbine engine. *Journal of Microelectromechanical Systems* 2000; **9**: 517–527.
18. Gupta AK, Lilley DG, Syred N. *Swirl Flows*, Abacus Press: Tunbridge Wells, Kent, 1984.
19. Yetter RA, Glassman I, Gabler HC. Asymmetric whirl combustion: a new low NOx approach. *Proceedings of Combustion Institute* 2000; **28**: 1265–1272.
20. Dasch CJ. One-dimensional tomography: a comparison of Abel, onion-peeling, and filtered backprojection methods. *Applied Optics* 1992; **31**: 1146–1152.

DOI: 10.1002/pip